# Reduction-of-Dimensionality Kinetics at Reaction-Limited Cell Surface Receptors

Daniel Axelrod*‡ and Michelle Dong Wang*
*Biophysics Research Division and ‡Department of Physics, University of Michigan, Ann Arbor, Michigan 48109

ABSTRACT It has been suggested for several years that reactions between ligands and cell surface receptors can be speeded up by nonspecific adsorption of the ligand to the cell surface followed by two-dimensional surface diffusion to the receptor, a mechanism referred to as "reduction-of-dimensionality" (RD) rate enhancement. Most of the theoretical treatments of this and related problems have assumed that the receptor is an irreversibly absorbing perfect sink. Such receptors induce a depletion zone of ligand probability density around themselves. The reaction rate in this case (called "diffusion-limited") is limited only by the time required for ligands to diffuse through this depletion zone. In some cases, however, the receptor may be far from "perfect" such that a collision with a ligand only rarely leads to binding. Receptors then do not create significant local depletion zones of ligand probability density, and the reaction rate becomes strongly affected by the (small) probability of reaction success per diffusive encounter (the "reaction-limited" case). This article presents a simple theory of RD rate enhancement for reaction-limited receptors that are either reversible or irreversible binders. In contrast to the diffusion-limited theories, the reaction-limited theory presented here: (*a*) differs quantitatively from diffusion-limited models; (*b*) is simple and algebraic in closed form; (*c*) exhibits significant rate enhancement in some realistic cases; (*d*) depends strongly on the actual Brownian rather than pure diffusive nature of the ligand's motion; (*e*) depends (for irreversibly binding receptors only) on the kinetic rates (not just equilibria) of reversible adsorption to nontarget regions, in contrast to some previous approximate theories of reduction of dimensionality; and (*f*) is applicable to actual ligand/receptor systems with binding success probabilities at the opposite extreme from the perfect sink/diffusion-limited models.

## INTRODUCTION

Since Adam and Delbruck (1968) hypothesized that reaction rates between solutes and membrane receptors can be enhanced by nonspecific solute adsorption and subsequent two-dimensional (2D) diffusion to the receptor, numerous theoretical and experimental works have attempted to clarify the relevance and magnitude of this enhancement in actual biochemical or biological systems (Berg and Purcell, 1977; Wang et al., 1992; Berg, 1985; Cukier, 1983; Burghardt and Axelrod, 1981; Thompson et al., 1981; Axelrod, 1983; Fulbright and Axelrod, 1993; McCloskey and Poo, 1986; Rhodes et al., 1985). This enhancement, by "reduction of dimensionality" (RD) from three-dimensional (3D) to 2D, might in principle contribute to the great sensitivity of some cells to low concentrations of ligands, and it also might provide practical clues on how to speed up reactions of immobilized enzymes in industrial applications.

Several models of ligand/cell surface receptor interactions (Berg and Purcell, 1977; DeLisi, 1980; Northrup, 1988; Zwanzig and Szabo, 1991; Baldo et al., 1991; Goldstein, 1989) assume that the receptor targets are permanent perfect sinks that can irreversibly absorb with infinite capacity any ligands that collide with them. As the target consumes ligand, it creates its own local concentration depletion zone, which then slows the observable reaction rates to a steady state. In a perfect sink theory, the ligand concentration right at the target is held equal to zero. The infinite capacity assumption does not well describe actual cell surface receptors, which are generally single-capacity and are continually replaced by fresh receptors. But even single-capacity receptors reside in statistical ligand depletion zones, apart from the very few that might appear on the surface in the immediate proximity of a ligand (Berg, 1978; Collins and Kimball, 1949), so theories based on infinite capacity sinks are still applicable.

On the other hand, a typical cell surface receptor may be "imperfect" in that only some small fraction of the Brownian collisions leads to binding. The ligand concentration at the target will generally be greater than zero and will approach the distant ligand concentration as the binding probability per collision approaches zero. The RD enhancement problem could be solved by the numerical methods of Wang et al. (1992) for a diffusion-limited perfect sink, except with an appropriately modified boundary condition for a "partial diffusion limited" sink (Collins and Kimball, 1949). However, in the limit of low binding probability, the solutions become much simpler and algebraically explicit and still show the effects of changing various parameters; this is the approach taken here. The low binding probability limit is called the "reaction-limit" because the speed of the reaction is limited by the low binding probability rather than the depleted local concentration. The zero-depletion zone/reaction-limit approach here is valid (at low binding probabilities) with only minor modifications for both irreversible and reversible reactions (such that a newly dissociated receptor may rebind the same or new ligand), but the results differ in several respects. Reversibility in ligand binding is seen in a variety of cell surface receptors, notably those for neurotransmitters.

*Received for publication 25 January 1993 and in final form 21 December 1993.*

Address reprint requests to Dr. Daniel Axelrod, Biophysics Research Division, University of Michigan, 930 N. University, Ann Arbor, MI 46109-1055.



0006-3495/94/03/588/13 $2.00

The perfect sink/diffusion-limited RD theory by Wang et al. (1992) itself was a significant modification of the Berg and Purcell (1977) theory, a theory that assumed equilibrium (rather than steady-state) adsorptive binding in the nontarget regions. Because of this difference, the theory of Wang et al. (1992) showed that the kinetic rate constants, and not just the equilibrium constant, of nontarget adsorption and desorption strongly affect the RD enhancement. The present article also shows the importance of these kinetic rate constants for irreversible reactions, but in addition shows that knowledge of the ligand's Brownian motion characteristic persistence length can be essential for predicting RD enhancement in some cases. Because the results of this paper for reaction-limited receptors differs quantitatively from that of Wang et al. (1992) for diffusion-limited receptors, we can conclude that the probability of reaction success per collisional encounter is a key parameter in determining the efficasy of RD enhancement.

## THE MODEL

Here we qualitatively consider questions of dimensionality, ligand reversibility, receptor distribution and ligand depletion zones, reaction probability, available receptor population, geometry, and microscopic details of the receptor/ligand interaction. (For general discussions of receptor ligand kinetics, see DeLisi (1983) and Lauffenburger and Linderman 1993).) We use the terms "target" as a more general substitute for "receptor"; "solute" as a more general substitute for "ligand"; "collision" for an encounter between a ligand and a target closer than some specified radius; and "reaction" for only those collisions that lead to ligand disappearance or inactivation (for irreversible reactions) or ligand detention (for reversible reactions).

### Dimensionality

In the RD system here, the kinetic processes in second and third dimensions are coupled so that reversible adsorption (characterized by adsorption and desorption rate constants $k_a$ and $k_d$) occurs only in nontarget ("nonspecific") regions. Specific targets embedded in the surface are assumed to be capable of binding solutes that approach from either 2D or 3D.

### Solute reversibility

In an irreversible reaction, the solute "disappears" once a reaction occurs. We assume it is replaced on the average by another solute molecule entering the system from an infinite reservoir far from the targets. In a reversible reaction, the solute binds to a specific target but then dissociates with some probability rate. Dissociated solutes would then be free to recollide and possibly (with some constant probability per collision) react again. The results for irreversible reactions can be applied as well to the reversible case, provided we reinterpret some of the variables.

### Target distribution and depletion zones

A biologically realistic picture should assume that the targets are single-capacity for ligands. In the reversible solute case, a target releases the solute unaltered after some time. In the irreversible solute case, two possibilities exist: a target/solute complex might "disappear" (e.g., by endocytosis) to be replaced (assumed instantaneously here) at some, possibly other, site by a fresh unbound target; or the solute may dissociate in an altered inactive form (e.g., as a product of a surface-bound enzyme), thereby leaving the target available for binding to another solute molecule.

Both the targets and the available solutes near and on the surface are presumed to be randomly distributed such that any small subarea or subvolume contains a Poisson-distributed number of targets and solutes, respectively. A random deletion of solutes and targets (e.g. by endocytosis after binding) will leave behind distributions that are still Poisson. Nevertheless, the relative distribution of solutes and targets is not random locally. Even in cases in which fresh targets appear randomly on the surface, some targets will be closer to solutes than others and those targets will likely react with solutes earlier. In this manner, the fact that a particular target may not have reacted for a "long time" (longer than a few tens of nanoseconds) is evidence that there are few solutes in its immediate vicinity. This local statistical depletion zone is just as real as if the target had been a steady state perfect sink with an infinite capacity and had annihilated the local solutes (Collins and Kimball, 1949; Berg, 1978). These local statistical depletion zones determine the reaction rate, even for single-capacity irreversible targets. The diffusion-limit/infinite sink RD enhancement theory of Wang et al. (1992) is thereby applicable even to diffusion-limit/single-capacity sinks. Likewise, the present reaction-limited theory is valid for both single capacity (with continual replacement) and infinite capacity (but permanent) targets.

For ease of calculation here, we approximate a random distribution of targets as a uniform one such that the targets are evenly spaced. Globally, irreversible targets on a cell surface will develop a depletion zone around the whole cell, of characteristic size on the order of the cell size. Solute molecules flow down the gradient of this global depletion zone, accounting for the rate at which the whole cell consumes solute.

For an equilibrated system with reversibly binding targets that remain on the surface, no global depletion zones will be present. However, local statistical depletion zones still exist around unoccupied targets for the same reason as discussed above. In fact, the diffusive flow (even at equilibrium) through this local depletion zone that accounts for the tendency of any group of purely unoccupied targets to become partially occupied over time.

### Reaction probability

The probability that any collision between an unoccupied target and a solute leads to a reaction affects the solute concentration in the local depletion zone proximal to the target. If the probability is unity, the local solute concentration ap-

proaches zero, creating a very deep depletion zone (the "diffusion-limit"). But if the reaction probability is sufficiently low (as discussed in Appendix A), the local concentration around each target can approach the solute concentration at regions near the cell surface that are more distant from any target, creating a very shallow depletion zone (the "reaction-limit"). Our simple algebraic approximation for RD enhancement assumes that the kinetic rate with the targets is reaction-limited.

### Population of available targets

For reversible targets, the total reaction rate from 2D and 3D affects the fraction of the targets that are unoccupied and thereby available for immediate reaction. But for those irreversible target reactions in which target/solute complexes disappear and new targets are incorporated into the cell surface, the population of available targets may be under some intracellular biochemical control that is sensitive to total reaction rate (e.g., "down-regulation"). For simplicity, in this case, we assume that the new incorporation is instantaneous after the disappearance of a bound complex (such that the new incorporation rate always equals the total reaction rate) and the number of available targets thereby remains a constant independent of total reaction rate. Last, for those irreversible target reactions in which the solute is held for a finite time and then released in an inactive form (e.g., enzyme/substrate systems), the number of available unoccupied targets will depend on the total reaction rate. Aside from pointing out where the theory can be modified to handle this case, we will not consider it further.

### Geometry

A common geometry for ligand/cell-surface receptor kinetics models consists of targets on a spherical cell of radius $A$. This geometry produces a steady state when the distant solute concentration is held at a finite constant. An alternative geometry consists of targets on an infinite flat plane, which for steady state requires a constant source concentration at some finite distance $H$ away. We show here that in the zero-depletion zone/reaction-limit, the math for the two geometries is formally identical: the sphere's radius $A$ is replaceable by the height $H$ in the equations.

### Microscopic details

Pure diffusion, with its fractal-like path, necessarily leads to an infinitely high collision rate for the situation here: a nonzero average solute concentration immediately in contact with each target. To account for finite reaction rates with nonzero local concentrations in pure diffusion, one must assume that the reaction probability per collision is diminishingly small (Collins and Kimball, 1949). Another approach recognizes that the molecules follow a Brownian motion path rather than pure diffusion; this approach yields a finite number of collisions/s from a finite solute concentration near a target. In Brownian motion, molecular velocity has a finite persistence length because the instantaneous momentum of the molecule can be transferred to the solvent at only a finite rate by solvent viscosity. The Brownian motion persistence length plays a central role in determining both reaction kinetic rates and the degree of RD enhancement in the present theory.

The effects of other molecular-scale features, such as the direction of approach and relative orientation of the reactants, and local electrical fields, are all compressed into the phenomenological constants of effective collision radius and probability of a reaction per collision.

## DEFINITIONS

We use notations somewhat similar to those of Wang et al. (1992).

### Diffusion coefficients

The diffusion coefficients used are: $D_3$ = bulk (3D) diffusion coefficient of solute ($cm^2/s$); and $D_2$ = surface (2D) diffusion coefficient of solute ($cm^2/s$).

### Nonspecific adsorption constants

The nonspecific adsorption constants are: $k_a$ = adsorption rate constant onto nontarget regions of the surface (cm/s); $k_d$ = desorption rate constant from nontarget regions of the surface ($s^{-1}$); and $K_e = k_a/k_d$ = adsorption equilibrium constant (cm).

Rate $k_a$ refers to the simple conversion of a bulk solute (at concentration $C_3$) into a nonspecifically adsorbed surface solute (at concentration $C_2$), represented by the chemical reaction

$$C_3 \xrightarrow{k_a} C_2.$$

Rate $k_a$ is implicitly proportional to the concentation of surface sites available for nonspecific binding and is thereby independent of solute concentration only if the adsorbate is far from saturating its surface sites. This formalism is slightly different from the definition of the corresponding $k_1$ rate of Thompson et al (1981) which explicitly takes into account the concentration of free surface sites $B$ through the reaction

$$C_3 + B \xrightarrow{k_1} C_2.$$

### Geometry

We assume that the targets are circular and uniformly spaced. Because of the uniform spacing, we assume each target sees the same solute environment as any other on the average and

therefore can be considered singly. Each target is positioned in the bottom center of its own exclusive volume domain with a bottom area corresponding to the target's share of the total surface area on the plane or the sphere. This assumption concerning the lateral position of the targets involves no loss of generality here because both the surface concentration and the bulk concentration proximal to the surface are laterally uniform in the reaction-limit. $R_a \equiv$ radius of a target (cm); and $R_b \equiv$ radius of the circular domain around the target (cm).

We consider either a spherical or flat geometry for the cell surface. For targets on a flat plane, a finite concentration solute source must be at a finite height above the surface to maintain a steady-state flow to the surface. For targets on a sphere, steady state can be maintained by a finite concentration source of molecules at infinity. $A \equiv$ radius of the sphere on which the circular targets reside; $H \equiv$ height measured from the flat plane on which the circular targets reside to the source plane.

In the spherical geometry, $R_b^2 = 4A^2/N$, where $N$ is the total number of available (unbound) targets on the cell.

### Solute concentrations

The relevant solute concentrations are: $C_0 \equiv$ 3D concentration at the solute source at the top of the domain (mol/cm$^3$) (at $r = \infty$ for a sphere and $z = H$ for a plane); $C_3 \equiv$ 3D concentration in the bulk immediately above the surface (mol/cm$^3$) (at $r = A$ for a sphere and $z = 0$ for a plane); and $C_2 \equiv$ 2D concentration on the surface (mol/cm$^2$).

Concentrations $C_3$ and $C_2$ are those that are "seen" locally by the target; we assume that neither is a function of lateral position in the target domain. This assumption makes the math simple but is accurate only in the case considered here: the limit of low probability of binding success upon collision ("reaction-limited"; see Appendix A).

### Collision rates and probabilities

A collision of a solute with a target is considered "successful" if the collision leads to a chemical reaction of interest. The relevant successful collision rates of solute per target (all in mol/s) are: $F_2 \equiv$ successful collision rate of nonspecifically adsorbed solute from 2D; and $F_3 \equiv$ successful collision rate of bulk solute directly from 3D.

The total reaction rate is:

$$F_t = F_2 + F_3 \tag{1}$$

$F_0 \equiv F_t$ evaluated at $D_2 = 0$ (i.e., no surface diffusion); $F_m \equiv$ maximum diffusion-limited rate per target, assuming the whole surface is a perfect sink; and $F_t$ cannot possibly be larger than $F_m$ for irreversibly binding targets. $\chi_{2,3} \equiv$ probabilities of reaction success per collision from 2D or 3D, respectively. These are denoted as $\chi$ in cases where $\chi_2 = \chi_3$.

### Brownian motion

$\sigma_{2,3} \equiv$ characteristic persistence distance of Brownian motion of the solute in 2D or 3D, respectively. $\sigma$ is related to the average radius of curvature in the Brownian path of the solute, or equivalently, to the characteristic decay distance of the Brownian motion velocity autocorrelation function. However, for simplicity, this distance has been approximated as a "jump" size in a random walk that simulates diffusion (Collins and Kimball, 1949; Noyes, 1954).

## EQUATIONS AND SOLUTIONS

First, we write expressions for $F_{2,3}$ in terms of the diffusion coefficients, local concentrations, and Brownian motion persistence lengths. One can show (Reif, 1965) that the number of collisions/s $\mathscr{F}_3$ of a Brownian solute at bulk concentration $C_3$ with a unit area surface is:

$$\mathscr{F}_3 = \langle \nu \rangle_3 C_3/4 \tag{2}$$

where $\langle \nu \rangle_3$ is the instantaneous speed of the Brownian solute in 3D averaged over the Maxwell distribution of speeds. The corresponding 2D expression for number of collisions/s $\mathscr{F}_2$ per unit length can be calculated in an analogous fashion, giving:

$$\mathscr{F}_2 = \langle \nu \rangle_2 C_2/\pi \tag{3}$$

In either dimensionality, speed $\langle \nu \rangle_n$ ($n = 2, 3$) is infinite for pure diffusion (as can be deduced from the diffusive displacement relationship $\langle x^2 \rangle = 2nDt$ or from the Maxwell mean square speed $kT/m$, where for a purely diffusing particle, mass $m \to 0$). But for Brownian motion, $\langle \nu \rangle_n$ is finite such that:

$$\langle \nu \rangle_n = \xi_n \sigma_n \tag{4}$$

where $\xi_n$ is the frequency of collisions experienced by a single particle and $\sigma_n$ is the free "run" between collisions. Strictly speaking, this relationship is appropriate for self-diffusion in gases, but the formalism has been applied (Collins and Kimball, 1949; Noyes, 1954) to Brownian motion where $\sigma_n$ is reinterpreted approximately as the Brownian persistence distance.

The effective diffusion coefficient $D_n$ in the appropriate dimensionality is:

$$D_n = \xi_n \sigma_n^2/2n \tag{5}$$

The reaction rates $F_{2,3}$ are found simply by multiplying the respective $\mathscr{F}_{2,3}$ rates of Eqs. 3 or 2 by success probabilities $\chi_{2,3}$ and by the circumference (for 2D) or the area (for 3D) of the circular target. Therefore, from Eqs. 1 through 3, we can write:

$$F_3 = (3\pi/2)\chi_3 R_a^2 D_3 C_3/\sigma_3 \tag{6}$$

$$F_2 = 8\chi_2 R_a D_2 C_2/\sigma_2 \tag{7}$$

The reaction rates $F_n$ are obviously strongly dependent on $\sigma_n$. As expected, the rates approach infinity in the pure

diffusion limit of $\sigma_n \rightarrow 0$ for finite $\chi_{2,3}$. Approximate values for $\sigma_n$ can be derived from the Langevin approach to Brownian motion (Reif, 1965; Russel, 1981). For very short times, the Brownian mean square displacement $\langle x^2 \rangle^{1/2} = (kT/m)^{1/2}t$ varies linearly with time $t$, and for very long times the Brownian displacement (for a spherical molecule) $\langle x^2 \rangle^{1/2} = (kT/3\pi\eta st)^{1/2}$ becomes diffusive and varies linearly with $t^{1/2}$, where $k$ = Boltzman's constant; $T$ = temperature; $\eta$ = viscosity; $m$ = molecular mass; and $s$ = molecular radius. By setting these displacement expressions equal, we can find an intermediate characteristic time, given by $t_c = m/3\pi\eta s$, around which the motion passes from predominantly linear to diffusive. The distance traveled in this characteristic time is then $\sigma_3 = \langle x^2 \rangle^{1/2}$ evaluated at $t_c$. Plugging in appropriate constants for $m$ and $s$ for a small peptide hormone and $\eta = 0.01$ p for the viscosity of water gives $\sigma_3 = 0.15$ Å. The effective viscosity in 2D on a biological membrane surface may be quite different from the 3D value. For the purposes of generating graphs of the solutions here, we will assume that $\sigma_2 = \sigma_3$. This assumption implies (from Eqs. 4 and 5) that any difference between $D_2$ and $D_3$ is accounted for entirely by a difference between collision frequencies $\xi_2$ and $\xi_3$. In general, however, knowing the ratio $D_3/D_2$ does not unambiguously determine $F_3/F_2$.

## Irreversible binding to targets

The "nonspecific" reversible binding to nontarget areas is characterized by association and dissociation kinetic rate constants $k_a$ and $k_d$, respectively. For irreversibly binding targets, every molecule that reacts with the target from 2D must have been previously adsorbed nonspecifically onto the surface from the bulk. Therefore, the net flow rate onto nontarget areas of the surface equals the irreversible 2D reaction rate with the target:

$$F_2^{irr} = \pi(R_b^2 - R_a^2)(k_a C_3 - k_d C_2) \quad (8)$$

(The superscript "irr" refers to the irreversible target version of the indicated variable). The factor involving $R_{a,b}$ is the nontarget area in the domain surrounding each target and accounts for the reaction rate as defined per target rather than per area.

In the case of infinite capacity targets, the rate of irreversible binding to a newly incorporated target in a sea of solutes typically shows a rapidly decaying initial transient as nearby ligands (if any are available) are captured, "eventually" (after tens of nanoseconds) reaching a steady state as more distant ligands flow down a local concentration probability density gradient toward the target. Even in the case of single capacity targets that disappear upon ligand binding and are replaced by fresh targets elsewhere, the situation is mathematically similar (for sufficiently low ligand concentrations, generally less than 1 M): we need only substitute the ligand concentration with the ligand probability density, and the ligand binding rate with a binding probability rate. But if $\chi_{2,3}$ are low, this local gradient of concentration (or probability density) can be quite flat, as discussed in Appendix A. In such a case, the only significant depletion zone is not a local one around each target as discussed above, but rather a global one between the membrane surface and distant regions of the bulk, formed by the combined effect of all the targets distributed on the surface. Regardless of whether the geometry is planar or spherical, the total reaction rate $F_t$ per target is equal to the flow rate of solute toward the target, and that flow rate is proportional to the difference between the bulk concentrations at a large distance $C_0$ and at the membrane surface $C_3$:

$$F_t^{irr} = \beta(C_0 - C_3) \quad (9)$$

For a planar geometry, the bulk concentration gradient and the flow rate are easily calculated from the diffusion equation and Fick's Law (and subsequently multiplying by the target domain area $\pi R_b^2$), yielding:

$$\beta_{plane} = \pi R_b^2 D_3/H \quad (10)$$

For a sphere, the flow toward the whole sphere is $4\pi A D_3(C_0 - C_3)$, so the flow per target can be easily written with:

$$\beta_{sphere} = \pi R_b^2 D_3/A \quad (11)$$

Factor $\beta$ is the only parameter in which the plane versus sphere question arises. Eqs. 10 and 11 show that $H$ of the planar geometry and $A$ of the spherical geometry should be interchangeable in the final results.

In the "enzyme/substrate" case where a bound target is unavailable for a certain finite time interval as the substrate is converted into a product, the number of available targets will depend on the total reaction rate. Hence the domain radius $R_b$ becomes a variable that itself depends upon $F_t^{irr}$. Although this complication can be still be handled algebraically in a straightforward fashion, for simplicity we only consider irreversible cases below in which $R_b$ is a fixed constant.

The five equations, Eq. 1 and Eqs. 6 through 9, are sufficient to solve for the five unknowns ($F_2$, $F_3$, $F_t$, $C_2$, $C_3$) in terms of all the other physical parameters ($R_{a,b}$, $H$ or $A$, $\sigma_{2,3}$, $k_{a,d}$, $D_{2,3}$, $\chi_{2,3}$) by elementary algebra. We express the results in terms of three functions of particular interest here.

(1) **2D fraction $f_2^{irr}$** is the ratio of the binding rate from the surface to the total binding rate:

$$f_2^{irr} \equiv F_2^{irr}/F_t^{irr} \quad (12)$$

We find that

$$f_2^{irr} = \left[\left(\frac{3\pi}{16}\right)\left(\frac{\sigma_2}{\sigma_3}\right)\left(\frac{\chi_3}{\chi_2}\right)\left(\frac{D_3}{D_2}\right)\left(\frac{R_a}{K_e}\right) \cdot\left(1 + \frac{8\chi_2 D_2 R_a}{\pi\sigma_2 k_d(R_b^2 - R_a^2)}\right) + 1\right]^{-1} \quad (13)$$

Fraction $f_3$ of solute arriving directly from the bulk is:

$$f_3^{irr} = 1 - f_2^{irr} \quad (14)$$

Clearly, $f_2^{irr}$ increases monotonically to a plateau as the nonspecific desorption kinetic rate constant $k_d$ increases, even as the nonspecific adsorption equilibrium constant $K_e$ is held fixed. Fig. 1 plots $f_2^{irr}$ versus $k_d$ for a particular reasonable set of parameters, for both the reaction-limited and diffusion-limited (Wang et al., 1992) cases. For the reaction-limited assumption to be valid given the choices of $R_{a,b}$ and $\sigma_{2,3}$, we must have $\chi \leq .001$: see Appendix A. We choose $\chi = .001$ for Fig. 1 *a*; smaller $\chi$ values shift the curves to the left without changing their shapes. At large enough $k_d$, collisions from 2D can completely dominate the collisional behavior, even for surface diffusion coefficients that are more than an order of magnitude less than the bulk diffusion coefficient.

As the target concentration increases ($R_b$ decreasing toward $R_a$), $f_2^{irr}$ approaches zero. As we proceed far into the reaction limit ($\chi_{2,3} \to 0$, while keeping $\chi_3/\chi_2$ constant), $f_2$ increases to a plateau that depends only on the equilibrium constant $K_e$ but not separately on the kinetic rate constant $k_d$. The radius of the whole cell $A$ (or the interplane spacing $H$) has no effect on f2irr.

(2) **RD factor $\eta^{irr}$** is the ratio by which a nonzero 2D

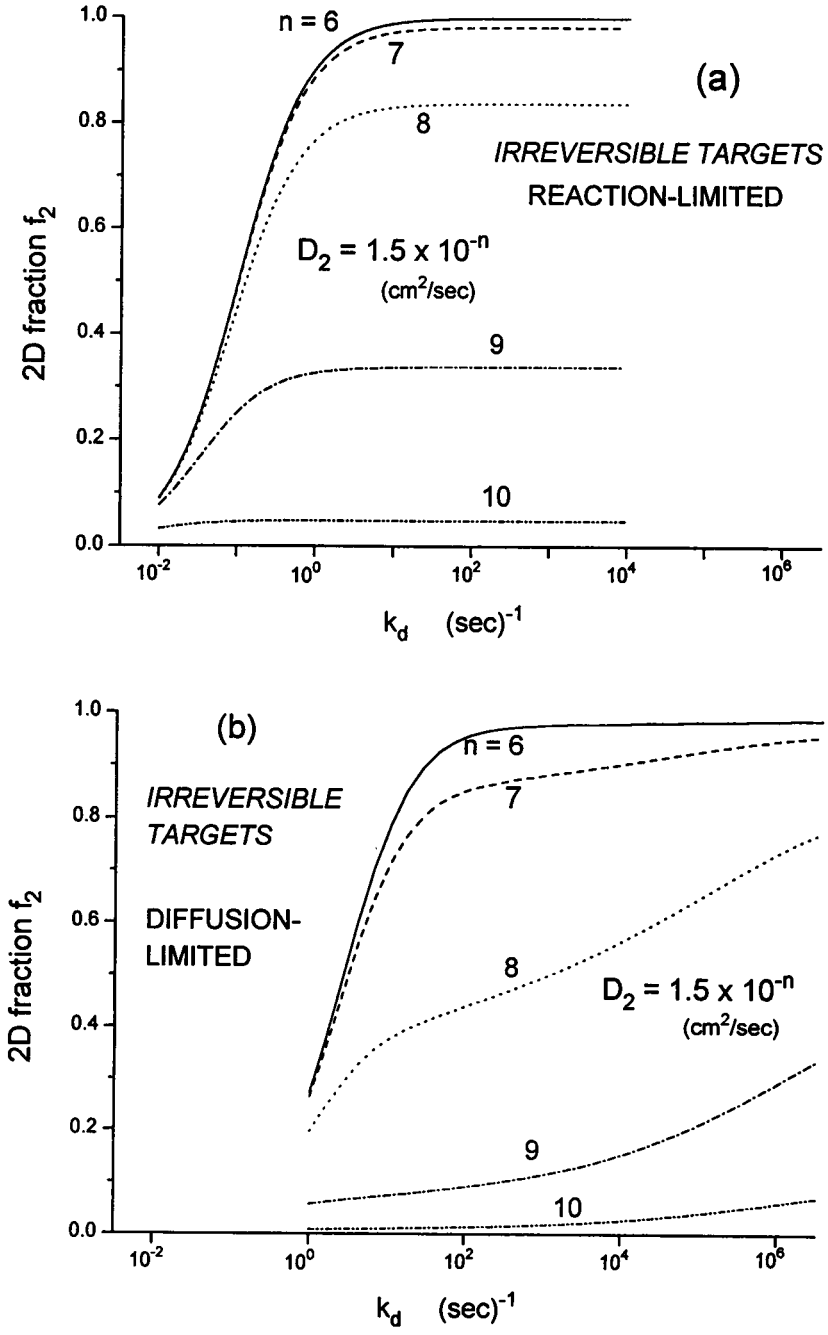


FIGURE 1 2D fraction $f_2$ as a function of nontarget desorption rate $k_d$ (in $s^{-1}$ and plotted on a log scale) for: (*a*) the reaction-limited irreversible model with Brownian parameters $\sigma_2 = \sigma_3 = 1.5 \times 10^{-9}$ cm and $\chi_2 = \chi_3 = .001$; and (*b*) the diffusion-limited (and planar) model of Wang et al. (1992). The diffusion-limited model curves were generated specifically for a planar geometry; the single capacity model easily interchanges between a plane and a sphere as discussed. In both cases, fixed parameters are: $R_a = 5 \times 10^{-8}$ cm; $R_b = 5 \times 10^{-5}$ cm; $A$ (or $H$) $= 5 \times 10^{-4}$ cm; $D_3 = 1.5 \times 10^{-6}$ $cm^2/s$; and $K_e = 1.5 \times 10^{-5}$ cm. Curves for surface diffusion coefficient $D_2 = 1.5 \times (10^{-6}, 10^{-7}, 10^{-8}, 10^{-9}$, and $10^{-10})$ $cm^2/s$ are shown as indicated.

diffusion coefficient enhances the total flow rate relative to what it would have been with $D_2 = 0$:

$$\eta^{irr} = F_t^{irr}/F_0^{irr} \tag{15}$$

$F_t^{irr}$ can be written as a function of $f_3^{irr}$:

$$F_t = \beta C_0 \left(1 + \frac{2f_3^{irr}\beta\sigma_3}{3\pi D_3 R_a^2 \chi_3}\right)^{-1} \tag{16}$$

$F_0^{irr}$ is simply $F_t^{irr}$ evaluated at $D_2 = 0$, which sets $f_3^{irr} = 1$. Therefore,

$$\eta^{irr} = \frac{1+q}{1+qf_3^{irr}} \tag{17}$$

where

$$q = \frac{2\beta\sigma_3}{3\pi D_3 R_a^2 \chi_3} \tag{18}$$

Fig. 2 plots $\eta^{irr}$ versus $k_d$ for the corresponding reaction-limited and diffusion-limited cases. The same parameters as in Fig. 1 are used in Fig. 2. RD enhancement $\eta^{irr}$ increases to a plateau with increasing $k_d$, even for a constant $K_e$. This effect, true for both the reaction-limited model and the diffusion-limited model, is in sharp distinction to the approximation of Berg and Purcell (1977), in which the rate enhancement depends only on the equilibrium constant, and the kinetic rates of nonspecific adsorption do not appear in the theory. At any particular $D_2$ and $k_d$, RD enhancement $\eta^{irr}$ increases with $K_e$ as all the curves of Fig. 2 expand upward and shift to the left.

As we proceed far into the reaction-limit ($\chi_{2,3} \to 0$ with $\chi_3/\chi_2$ constant), $\eta^{irr}$ approaches a limiting value for any particular set of parameters. For the constant values of $D_3$, $\sigma_{2,3}$, $R_a$, and $K_e$ used in the figures, $\eta^{irr}$ can be quite substantial, ranging from severalfold to several hundredfold for $D_2$ ranging from $= 1.5 \times 10^{-8}$ to $1.5 \times 10^{-6}$ (cm$^2$/s).

Fig. 3 *a* shows how $\eta^{irr}$ varies with the intertarget spacing $R_b$, which increases with decreasing target concentration. RD enhancement $\eta^{irr}$ increases monotonically from unity (at high target concentration) to $1/f_3^{irr}$ (at low target concentration).

(3) **Global efficiency $\gamma^{irr}$** compares the total flow rate per target $F_t$ with the flow rate per target $F_m$ that would occur if the entire membrane surface were a perfect sink.

$$\gamma^{irr} \equiv F_t^{irr}/F_m \tag{19}$$

$F_m$ equals $\beta C_0$, as can be seen by setting $C_3 = 0$ (the perfect sink boundary condition in Eq. 9). From Eq. 16, we get:

$$\gamma^{irr} = \left(1 + \frac{2f_3^{irr}\beta\sigma_3}{3\pi D_3 R_a^2 \chi_3}\right)^{-1} \tag{20}$$

Fig. 3 *b* shows how $\gamma$ varies with target concentration. It shows that the whole cell can behave as a perfect sink even if the small targets on its surface are highly imperfect, reaction-limited sinks. Evidently, a solute molecule can collide often enough with targets while in the vicinity of the cell surface to overcome the low reaction probability per collision; it will eventually be consumed with high probability by some target. As long as the conditions for reaction-limit are met (Appendix A), a deep global depletion zone can exist even when local depletion zones are very shallow. This behavior is a generalization of the Berg and Purcell (1977) conclusion that even a low concentration of small perfect sink targets uniformly distributed on a spherical cell could make the whole cell appear as a perfect sink to the environment.

Global efficiency $\gamma$, RD enhancement $\eta$, and 2D fraction $f_2$ are related by:

$$\eta^{irr} = \gamma^{irr} + \frac{1-\gamma^{irr}}{1-f_2^{irr}} \tag{21}$$

## Reversible binding to targets

The theory in the previous subsection treats the targets as irreversible sinks. What if the targets are not sinks at all but can bind ligands reversibly? In such a case, we might assume that each binding leads to some physiological effect, but the ligand is unaltered and is free to rebind any time after dissociation from the target. The flow rate of solute toward the targets, averaged over all targets—both bound and unbound—is zero. But the flow rate toward just the unbound targets is not zero; these available targets reside in statistical depletion zones as evidenced by the fact that they are unbound. As for the irreversible case, this depletion zone is very shallow if the reaction probabilities $\chi_{2,3} \ll 1$, and the same overall simple algebraic approach should still be applicable. The system is not just in steady state, but in equilibrium, so that the nontarget adsorption kinetic rates $k_a$ and $k_d$ will act only in their ratio $K_e$ which then also equals the surface/bulk concentration ratio $C_2/C_3$.

In the reversible target case, the number of available unbound targets on the cell surface depends on the specific binding and dissociation rates at the targets: the ratio of these rates determines the equilibrium fraction $\alpha$ of unbound versus total targets. The reaction-limited binding rate per unbound target is $F_2 + F_3$; the dissociation rate per bound target is given by $\tau^{-1}$ where $\tau$ is the mean time that a target holds its ligand before randomly releasing it. Fraction $\alpha$ can be easily calculated to be:

$$\alpha = \left[\tau R_a C_3 \left(\frac{8\chi_2 D_2 K_e}{\sigma_2} + \frac{3\pi\chi_3 R_a D_3}{2\sigma_3}\right) + 1\right]^{-1} \tag{22}$$

The average binding rates per target (averaged over all targets both bound and unbound) are then $\langle F_{2,3,t}\rangle = \alpha F_{2,3,t}$. It is true that $R_b$ becomes a variable as the number of available sites changes, as in the irreversible "enzyme/substrate" case discussed earlier. But here in the reversible target case, $R_b$ does not enter into the calculations. We now calculate for the reaction-limited reversible case the analogous variables to those of the reaction-limited irreversible case above.

(1) **2D fraction $\langle f_2^{rev}\rangle$.** In the reversible case, the reaction rate $\langle F_t\rangle$ analogous to Eq. 1 is no longer equal to the net flow toward the surface as in the irreversible case $F_t^{irr}$ (Eq. 9);

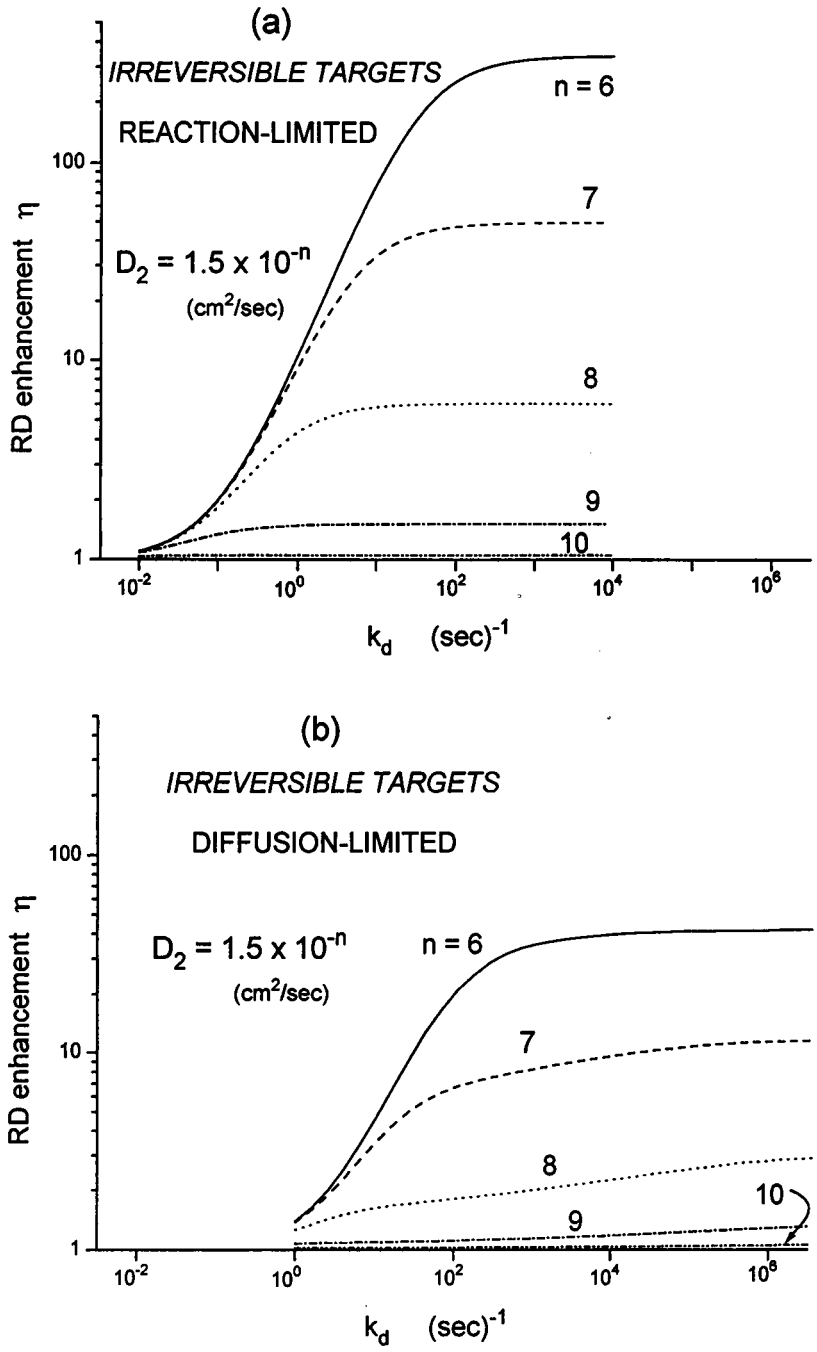


FIGURE 2 RD factor $\eta$ as a function of nontarget desorption rate $k_d$ (in $s^{-1}$, plotted on a log scale) for: (*a*) the reaction-limited irreversible model; and (*b*) the diffusion-limited (and planar) model of Wang et al. (1992). The same parameters are used as in Fig. 1.

indeed, the net flow is zero for reversible binding. The rates $\langle F_{2,3} \rangle$ are given by Eqs. 6 and 7, each multiplied by $\alpha$, but they are entirely decoupled because bulk concentration $C_3$ near the surface is constant and equals the distance bulk concentration $C_0$ under all conditions. The solution for $\langle f_2^{rev} \rangle$ ($\equiv \langle F_2 \rangle / \langle F_t \rangle = 1 - \langle f_3^{rev} \rangle$) is then:

$$\langle f_2^{rev} \rangle = \left[ \left( \frac{3\pi}{16} \right) \left( \frac{\sigma_2}{\sigma_3} \right) \left( \frac{\chi_3}{\chi_2} \right) \left( \frac{D_3}{D_2} \right) \left( \frac{R_a}{K_e} \right) + 1 \right]^{-1} \quad (23)$$

Note that $\langle f_2^{rev} \rangle$ does not depend on $C_3$, nor $\tau$, nor the unbound fraction $\alpha$, nor the intertarget spacing $R_b$. $\langle f_2^{rev} \rangle$ is identical with the asymptotic limits ($\chi_{2,3} \to 0$ for constant $\chi_3/\chi_2$, or $k_d \to \infty$ for constant $K_e$) of $f_2^{irr}$.

(2) **RD factor** $\langle \eta^{rev} \rangle$ ($\equiv \langle F_t^{rev} \rangle / \langle F_0^{rev} \rangle$) is affected by the dependence of the free target fraction $\alpha$ on $D_2$. If $D_2 = 0$, then $\alpha$ increases to the value $\alpha_0$. We find that:

$$\langle \eta^{rev} \rangle = (\alpha/\alpha_0)(1/\langle f_3^{rev} \rangle) \quad (24)$$

$\langle \eta^{rev} \rangle$ is a strong function of the bulk concentration $C_3$, unlike $\eta^{irr}$ (Eq. 27) which is independent of $C_3$. The reason for this difference is that, in the reversible case, the number of available reversible receptors decreases as the specific binding rates increase (for the same characteristic binding time $\tau$), but in our irreversible cases, the number of available receptors is unaffected by binding rates. Fig. 4

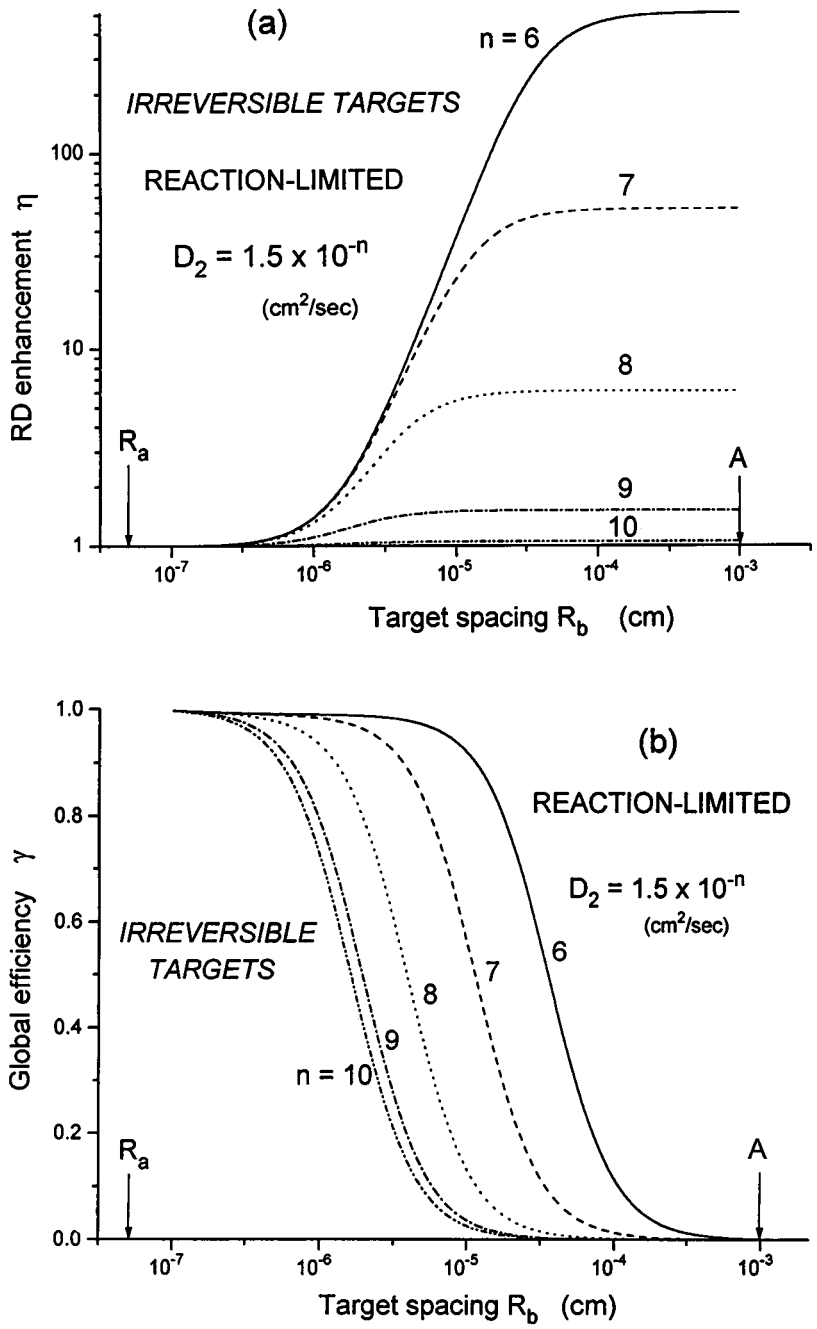


FIGURE 3 The effect of intertarget spacing distance $R_b$ on: (*a*) RD factor; and (*b*) global efficiency factor $\gamma$ for irreversible reaction-limited targets. Target concentration decreases toward the right. The same parameters are used as in Figs. 1 and 2 except that $k_d$ is fixed at $1 \times 10^4$ s$^{-1}$ and $R_b$ is made variable over almost the entire range from the target radius $R_a$ to the cell radius $A$, as indicated on the abscissa.

shows $\langle \eta^{rev} \rangle$ plotted against the product $\chi\tau C_3$ for parameters similar to those used to calculate $\eta^{irr}$ in Fig. 3. The potential RD enhancement can be very substantial for quite reasonable physiological values of $\chi\tau C_3$ and $D_2$. The appearance of the product $\chi\tau C_3$ shows that a decrease in any of those three factors can be compensated by an increase in the others. $\langle \eta^{rev} \rangle$ is not a function of the kinetic rate constants $k_a$ and $k_d$ separately (as is $\eta^{irr}$) but only of the nonspecific adsorption equilibrium constant $K_e$, as would be expected from an equilibrium process.

(3) **Global efficiency** $\langle \gamma^{rev} \rangle$ compares the average total reversible reaction rate per target ($\langle F_t^{rev} \rangle = \alpha F_t^{rev}$) with the highest possible total irreversible reaction rate per target $F_m$ ($= \beta C_0$) as can be attained by a surface covered by perfect sink targets.

$$\langle \gamma^{rev} \rangle \equiv \langle F_t^{rev} \rangle / F_m \tag{25}$$

For reversible targets, there is no global depletion zone, so $C_0 = C_3$ and $F_m = \beta C_3$. In general, $\langle \gamma^{rev} \rangle$ is linearly proportional to the target concentration and can be orders of magnitude larger than unity at the higher target densities ($R_b \rightarrow R_a$). The reason why reversible reactions are so "efficient" is that the solute can rebind repeatedly without having to diffuse through a global depletion zone, as in the irreversible case.

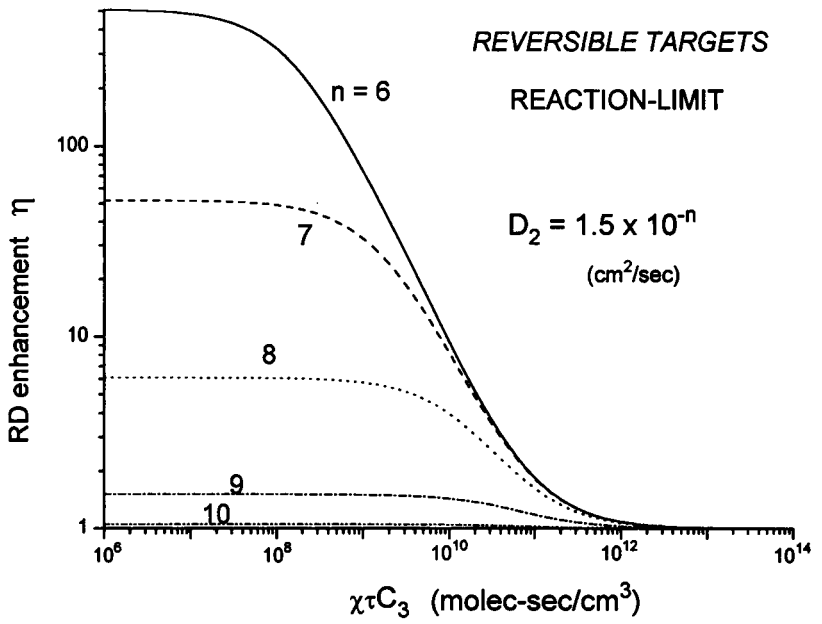


FIGURE 4 Average RD factor $\langle \eta^{rev} \rangle$ as a function of the product $\chi\tau C_3$ for targets that bind solutes reversibly. The same parameters are used as in Fig. 1, where relevant.

## DISCUSSION

The theory presented here for RD enhancement toward reaction-limited targets, both irreversible and reversible, is an extension of that presented by Wang et al. (1992) for irreversible diffusion-limited/perfect sinks. The present model is simple and algebraic because here it assumes that no significant local depletion zones develop around any targets. This assumption is approximately true if binding occurs only with low probability on each collision, as discussed in Appendix A. A distinct difference between this reaction-limited model and the diffusion-limited model for irreversible targets is the strong dependence of RD enhancement on the reaction probabilities $\chi_{2,3}$. A general model of RD enhancement for partial-diffusion-limited irreversible sinks has not yet appeared, but would almost certainly require a numerical solution on a computer. Such a model would follow the approach of Wang et al. (1992) except that the solute concentration boundary condition at the surface of a target would be set as the "partial reflection" condition of Collins and Kimball (1949) (their Eq. 28) rather than set at zero.

The constant parameters used in the Figs. 1 through 3 for the reaction-limited irreversible target case were chosen to be biophysically reasonable. $R_a$ = 5 A is a value typically used in Smoluchowski theory calculations (DeLisi, 1980). $\sigma_3$ = 0.15 Å comes from our Brownian motion approximation for a solute molecule with a molecular weight of 3000 and effective spherical radius of 10 Å dissolved in water. $\sigma_2$ was set equal to $\sigma_3$ although the actual value probably depends greatly on the detailed molecular environment of the surface. $A$ was set equal to 5 $\mu$m, typical of a lymphocyte. $R_b$ was set at 0.5 $\mu$m so that the total number of targets per cell is set at 400, which is sufficiently small for 2D diffusion to have a chance to increase the total collision rate (see Fig. 3 *a*). The $K_e$ was set to the value ($1.5 \times 10^{-5}$ cm) found for nonspecific adsorption of insulin on erythrocyte membrane (Fulbright and Axelrod, 1993). Reaction probabilities $\chi_{2,3}$ were set at .001 to ensure we are in the reaction-limit (see Appendix A). These reasonable parameters result in substantial RD enhancement factors $\eta^{irr}$, ranging from 1.5 to 337, for $D_2 = 1.5 \times 10^{-9}$ to $1.5 \times 10^{-6}$ (cm$^2$/s), respectively, for $k_d > 10^4$ s$^{-1}$.

For any particular desorption rate constant, $k_d$, stronger equilibrium binding as measured by $K_e$ leads to a greater 2D enhancement factor $\eta$. Increasing $K_e$ for a constant $k_d$ means increasing $k_a$; evidently, more adsorptions (and desorptions)/s of solute at nontarget regions lead to a greater enhancement of the reaction rate with the targets. Nonetheless, there is a limit to how large the adsorption rate $k_a$ can be. In analogy with Eq. 6 which concerns target reactions, the number of collisions/s $F_3'$ with the *non*target region of the surface in each target domain is:

$$F_3' = (3\pi/2)(R_b^2 - R_a^2)D_3C_3/\sigma_3 \qquad (26)$$

At the maximum possible adsorption rate, all of these collisions would lead to adsorption. We then can set $F_3'$ equal to the adsorption rate term analogous to that in Eq. 8, $\pi(R_b^2 - R_a^2)\, k_a^{max}C_3$, thereby giving:

$$k_a^{max} = (3/2)D_3/\sigma_3 \qquad (27)$$

For the values of $D_3$ and $\sigma_3$ used previously, this gives $k_a^{max}$ = 2250 cm/s. For any $K_e$, this maximal diffusion-limited $k_a^{max}$ then determines the maximal possible desorption rate $k_d^{max}$. For our parameters with $K_e = 1.5 \times 10^{-5}$ cm, we get $k_d^{max} = 1.5 \times 10^8$ s$^{-1}$. Because this maximal value is larger than any plotted in the abscissa of Fig. 2, the range shown there is physically reasonable. Given an actual $k_a$ value obtained from experimentally measured $k_d$ and $K_e$ values, we can also calculate the ratio $k_a/k_a^{max}$, which is the probability that *non*target collisions will result in adsorption. This probability can be remarkably small (as

small as $10^{-7}$ for the chosen parameters, four orders of magnitude yet smaller than the already-small probabilities of success for on-target reaction-limited collisions) and still yield a significant RD enhancement over the zero surface diffusion case.

A significant approximation in the approach presented here is the substitution of a mean-free-path model of molecular motion in place of a more accurate formulation of Brownian motion in a liquid. This approximation probably does not affect the trends, but it will affect the absolute magnitudes chosen for the $\sigma_{2,3}$ lengths. Because we do not know what the exact value of $\sigma_2$ should be, it is interesting to see what happens when it is varied. For both the reversible and irreversible reaction-limited cases considered here, RD enhancement $\eta$ increases as $\sigma_2$ decreases (while $D_2$ is held constant). A smaller $\sigma_2$ corresponds to sharper twists and turns in the random walk of Brownian motion and thereby to more collisions/s in 2D. In both the reversible and irreversible models here, decreasing $\sigma_3$ toward zero (the pure diffusion limit) suppresses the RD enhancement factor down toward unity, at which value 2D diffusion could not possibly enhance reaction rates.

The strong dependence of all the results on $\sigma_{2,3}$ parameters which do not even appear in pure diffusion theories (e.g., Berg and Purcell, 1977; Collins and Kimball, 1949), seems at first to raise a question about the relevance of pure diffusion theories. However, in situations in which depletion zones are relevant (non-reaction-limited targets), pure diffusion theories become applicable when the characteristic size of the depletion zone becomes much larger than the Brownian persistence distances $\sigma_{2,3}$ and the former thereby becomes the relevant characteristic distance in the problem.

It is entirely possible that the reaction probabilities are not the same for both the 2D and 3D routes; i.e., $\chi_2 \neq \chi_3$. In particular, what if the probability $\chi_2 = 0$ but $\chi_3 > 0$? According to Eq. 7, the effect would be exactly the same as if $D_2$ were zero; i.e., surface diffusion could not possibly lead to reaction rate enhancement. This conclusion is in contradistinction to the diffusion-limited model, where the depth and shape of the local depletion zone in 3D can be affected by 2D diffusion, even if no reactions occur directly from 2D (see Appendix B).

Our calculations show that RD enhancement can be substantial for reaction-limited cell surface targets. But the magnitude of the predicted RD enhancement depends on a variety of molecular details of the reactions beyond those considered by the approximate Berg and Purcell theory. These features are characterized by: Brownian distances $\sigma_2$ and $\sigma_3$; nonspecific kinetic rate constants $k_a$ and $k_d$ separately; the position of the specific reaction on the spectrum between diffusion- and reaction-limited rates; whether the reaction can occur by collision from both 2D and 3D or from 3D only, or perhaps in a guided 3D manner (as suggested by Tan et al., 1993); whether or not reversible nonspecific adsorption occurs at the receptive patches themselves (e.g., Berg, 1985); and whether the targets are reversible or irreversible.

## APPENDIX A

### The reaction-limit and $\chi$

For the simple algebraic approach to kinetic rates in this article to be valid, the local concentrations $C_2$ and $C_3$ around a target must not vary much with distance from the target, at least out to a distance on the order of the intertarget radius $R_b$. To obtain very approximate expressions for $\chi_{2,3}$ for which this condition will be true, we will divide the problem into pure 3D and pure 2D aspects.

In 3D, we can approximate each target as a partially absorbing spherical sink of radius $R_a$ (rather than a disk of the same radius). The distant concentration (at $r \sim R_b$) is $C_3'$, and the concentration at the surface of the target (necessarily less than $C_3'$) is designated as $C_3$. We want the ratio $C_3'/C_3$ to be only slightly larger than unity; this situation corresponds to the almost flat local concentration profile that defines the "reaction-limit." In steady state, both $C_3$ and $C_3'$ are constant in time and the flow rate $F_3$ into one hemisphere (corresponding to the target surface facing out from the membrane) has the form:

$$F_3 = \frac{2\pi D_3 R_a (C_3' - C_3)}{1 - (R_a/R_b)} \tag{A1}$$

This flow rate can also be described by a kinetic formula analogous to Eq. 6 (except modified for the area of a hemisphere instead of a disk):

$$F_3 = 3\pi\chi_3 R_a^2 D_3 C_3/\sigma_3 \tag{A2}$$

Setting these two expressions equal, noting that $R_a/R_b \ll 1$, and solving for $\chi_3$ gives:

$$\chi_3 = \left(\frac{2}{3}\right)\left(\frac{C_3'}{C_3} - 1\right)\left(\frac{\sigma_3}{R_a}\right) \tag{A3}$$

If, for example, we demand that the proximal and more distal local concentrations $C_3$ and $C_3'$ differ by no more than 10%, then $C_3'/C_3 = 1.1$. For reasonable values of $\sigma_3$ ( $= .15 \times 10^{-8}$ cm) and $R_a$ ($= 5 \times 10^{-8}$ cm), we then conclude that $\chi_3$ must be $\leq .002$ for a maximum of 10% inaccuracy in the zero local depletion zone assumption.

Likewise in 2D, we model the target domain as a circular source at $r = R_b$ maintained at a steady state concentration of $C_2'$, surrounding a partial sink of radius $r = R_a$ with a concentration of $C_2$ at its circumference. In this simplified geometry, one can easily show from the diffusion equation that:

$$F_2 = \frac{2\pi D_2 (C_2' - C_2)}{\ln(R_b/R_a)} \tag{A4}$$

The kinetic expression for $F_2$ analogous to that of Eq. 7 is:

$$F_2 = 8\chi_2 R_a D_2 C_2/\sigma_2 \tag{A5}$$

Equating these two expressions and solving for $C_2$ gives:

$$\chi_2 = \left(\frac{\pi}{4}\right)[\ln(R_b/R_a)]^{-1}\left(\frac{C_2}{C_2'} - 1\right)\left(\frac{\sigma_2}{R_a}\right) \tag{A6}$$

Reasonable values for the reciprocal log term would extend from about 2 to about 1/9, thereby covering a wide range (eight orders of magnitude) of target concentrations. Substituting in $\sigma_2$ (= .15 × $10^{-8}$ cm), $R_a$ (= 5 × $10^{-8}$ cm), and $R_b$ = 1000 $R_a$, we conclude that a maximum of 10% inaccuracy in the 2D local zero depletion zone asumption requires that $\chi_3 < .001$.

In the actual RD enhancement problem, the 2D and 3D regimes interact via the nonspecific reversible adsorption route. But if we choose both $\chi_2$ and $\chi_3$ to equal the lesser of the $\chi_{2,3}$ values estimated here (.001), it can be shown (by an electric resistor network circuit analogy, unpublished) that "turning on" the 2D/3D interaction depletion zone will not significantly deepen the local 3D depletion zone beyond 10% while somewhat filling the 2D depletion zone.

The simplified model above also overestimates local depletion zones because it places the sources for new solute exclusively at $R_b$, far from each target. A model more representative of the actual RD enhancement problem would spatially distribute the sources over the whole ring area between $R_a$ and $R_b$, corresponding to 3D diffusion from distal regions and adsorption onto the surface.

## APPENDIX B

## Boundary conditions

### *Perfect sink model: what happens if reactions can only occur from 3D?*

An actual membrane receptor probably binds ligands which approach the active site from within some limited solid angle. In one interesting limit, the active site might be viewed as a target that only accepts ligands approaching from 3D, and not directly from 2D at all. For a reaction-limited model in a such a situation, we have shown that a 2D reaction rate enhancement does not occur. But for a diffusion-limited model, the effect is different. The local 3D depletion zone will give rise (through nonspecific adsorption kinetics) to a local 2D depletion zone, through which 2D-adsorbed ligands can flow toward the target in steady state. For a reaction to occur, desorption near the target is required; this will tend to partially fill the local 3D depletion zone and thereby enhance reaction rates over what they would have been in the absence of nonspecific adsorption and/or surface diffusion. Even so, one would not expect this mode of approach to make any difference if the adsorption/desorption rates $k_a$ and $k_d$ are (*a*) so very fast that the bulk and the surface are essentially in equilibrium; or (*b*) so very slow that desorption near the target can only negligibly augment 3D diffusion toward the target. But for intermediate kinetic rates (presumably for $k_d$ rates comparable to the rate of 3D diffusion through the 3D depletion zone), 2D enhancement might occur.

We have tested this hypothesis using the same steady-state perfect sink program as in Wang et al. (1992) but with one change: the 2D perfect sink boundary condition $C_2(r = R_a) = 0$ is here replaced with a 2D perfect reflecting boundary condition $\partial C/\partial r(r = R_a) = 0$. The result confirms that RD enhancement can occur, but (for the same input parameters as in the solid curve of Fig. 3 *b*), it does not become significant (>1.2) until $k_d$ is greater than 1 × $10^6$ $s^{-1}$, a very high desorption rate constant. Therefore, in most situations, 2D enhancement is much more likely to be important if the target can capture ligands directly from 2D. The great sensitivity in the results to this detail concerning the ligand's final direction of approach should be studied in less extreme and effectively intermediate models; e.g., in which a graded potential attracts ligands to a zone near the surface through which ligands diffuse in 3D but with a bias toward remaining near the surface.

### *The most general approach*

The perfect 2D sink diffusion boundary [$C_2(r = R_a) = 0$], the perfect 2D reflecting diffusion boundary [$\partial C_2/\partial r (r = R_a) = 0$], and the reaction-limit approximation [$C_2$ independent of $r$] used here are all special cases of the general Collins and Kimball (1949) partial reflection boundary [$D_2\partial C_2/\partial r(r = R_a) = kC_2(r = R_a)$, where $k$ is an intrinsic rate of specific binding such that $k = (4/\pi)(\chi D_2/\sigma_2)$ in our notation]. (Analogous expressions for 3D can be easily written.) For a perfect sink in pure diffusion, $\chi = 1$ and $\sigma_2 \to 0$ so $k \to \infty$. For the perfect reflecting boundary in pure diffusion, $\chi = 0$ and $\sigma_2 \to 0$ so $k = 0$. For the reaction-limit, $\chi \to 0$ so $k \to 0$, which forces $\partial C_2/\partial r(r = R_a) \to 0$ and thereby yields an increasingly flat $C_2$ almost independent of $r$. A completely general (numerical) solution of the RD enhancement problem should start with the Collins and Kimball condition.

We thank Dr. Nancy Thompson for very helpful discussions on this and related topics in chemical kinetics and one of the reviewers for important comments on the nature of statistical depletion zones.
This work was supported by the National Institutes of Health (NS14565) and the National Science Foundation (DMB8805296).

## REFERENCES

Adam, G., and M. Delbruck. 1968. Reduction of dimensionality in biological diffusion processes. *In* Structural Chemistry and Molecular Biology. A. Rich and N. Davidson, editors. W. H. Freeman and Company, San Francisco. 198–215.

Axelrod, D. 1983. Lateral motion of membrane proteins and biological function. *J. Membr. Biol.* 75:1–10.

Baldo, M., A. Grassi, and A. Raudino. 1991. Diffusion-controlled reactions among ligands and receptor clusters. Effects of competition for ligands. *J. Chem. Phys.* 95:6734–6740.

Berg, H., and E. M. Purcell. 1977. Physics of chemoreception. *Biophys. J.* 20:193–239.

Berg, O. 1978. On diffusion-controlled dissociation. *Chem. Phys.* 31:47–57.

Berg, O. 1985. Orientation constraints in diffusion-limited macromolecular association. The role of surface diffusion as a rate-enhancing mechanism. *Biophys. J.* 47:1–14.

Burghardt, T. P., and D. Axelrod. 1981. Total internal reflection/fluorescence photobleaching recovery study of serum albumin adsorption dynamics. *Biophys. J.* 33:455–468.

Collins, F. C., and G. E. Kimball. 1949. Diffusion-controlled reaction rates. *J. Colloid Sci.* 4:425–437.

Cukier, R. I. 1983. The effect of surface diffusion on surface reaction rates. *J. Chem. Phys.* 79:2430–2435.

DeLisi, C. 1980. The biophysics of ligand-receptor interactions. *Q. Rev. Biophys.* 13:201–230.

DeLisi, C. 1983. Stochastic problems in information transfer across the plasma membrane. *Bull. Math. Biol.* 45:467–482.

Fulbright, R. M., and D. Axelrod. 1993. Dynamics of nonspecific adsorption of insulin to erythrocyte membrane. *J. Fluor.* 3:1-16.

Goldstein, B. 1989. Diffusion-limited effects of receptor clustering. *Comm. Theor. Biol.* 1:109–127.

Lauffenburger, D. A., and J. J. Linderman. 1993. Receptors: Models for Binding, Trafficking, and Signalling and their Relationship to Cell Function. Oxford University Press, New York.

McCloskey, M. A., and M-M. Poo. 1986. Rates of membrane-associated reactions: reduction of dimensionality revisited. *J. Cell. Biol.* 102:88–96.

Northrup, S. H. 1988. Diffusion-controlled ligand binding to multiple competing cell-bound receptors. *J. Chem. Phys.* 92:5847–5850.

Noyes, R. M. 1954. A treatment of chemical kinetics with special applicability to diffusion controlled reactions. *J. Chem. Phys.* 22:1349–1359.

Reif, F. 1965. Fundamentals of Statistical and Thermal Physics. McGraw-Hill, New York. 651 pp.

Rhodes, D. G., J. G. Sarmiento, and L. G. Herbette. 1985. Kinetics of binding of membrane-active drugs to receptor sites. Diffusion-limited rates for a membrane bilayer approach of 1,4-dihydropyridine calcium channel agonists to their active site. *Mol. Pharmacol.* 27:612–623.

Russel, W. B. 1981. Brownian motion of small particles suspended in liquids. *Annu. Rev. Fluid Mech.* 13:425–455.

Tan, R. C., T. N. Truong, and J. A. McCammon. 1993. Acetylcholinesterase: electrostatic steering increases the rate of ligand binding. *Biochemistry.* 32:401–403.

Thompson, N. L., T. P. Burghardt, and D. Axelrod. 1981. Measuring surface dynamics of biomolecules by total internal reflection with photobleaching recovery or correlation spectroscopy. *Biophys. J.* 33:435–454.

Wang, D., S-Y. Gou, and D. Axelrod. 1992. Reaction rate enhancement by surface diffusion of adsorbates. *Biophys. Chem.* 43:117–137.

Zwanzig, R., and A. Szabo. 1991. Time dependent rate of diffusion-influenced ligand binding to receptors on cell surfaces. *Biophys. J.* 60: 671–678.